

Bis(*p*-aminobenzoato)bis(hexadecanoato)dicopper(II): A low-temperature and thermally-stable functional metallomesogen

 Ahmad Nazeer Che Mat ^{a,*}, Mohammad Isa Mohamadin ^b
^a Department of Chemistry, Faculty of Science, University of Malaya, 50603 Kuala Lumpur, Malaysia

^b Faculty of Applied Sciences, Universiti Teknologi MARA, 94300 Kota Samarahan, Sarawak, Malaysia

* Corresponding author: hmd_naz@yahoo.com

Article history

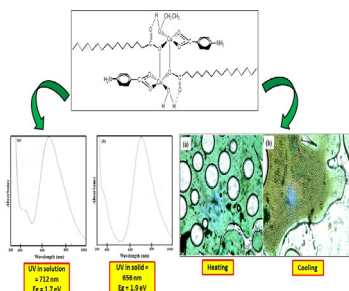
Received 25 May 2020

Revised 20 July 2020

Accepted 12 August 2020

Published Online 24 December 2020

Graphical abstract



Abstract

A novel copper (II) mixed carboxylates namely bis(*p*-aminobenzoato)bis(hexadecanoato)dicopper(II), [Cu₂(*p*-H₂NC₆H₄COO)₂(CH₃(CH₂)₁₄COO)₂], from one-pot self-assembly of the corresponding ions was designed to function as a low-temperature and thermally-stable metallomesogen applications. The as-prepared copper (II) complex was characterized by means of CHNS analysis, Fourier Transform Infrared (FTIR) spectroscopy, Ultraviolet-Visible (UV-Vis) spectroscopy, thermogravimetric analysis (TGA), differential scanning calorimetry (DSC), optical polarized microscopy (OPM), magnetic Gouy balance, and cyclic voltammetry (CV) for the determination of its elemental compositions, chemical bonding, optical properties, thermal stability, phase transition, magnetic properties and electrochemical behavior of the complex, respectively. Its melting and decomposition temperatures are 115 °C and 256 °C, respectively, and formed a smectic C mesophase on cooling from the isotropic liquid phase. Its room-temperature effective magnetic moment is 2.89 B.M., indicating a paramagnetic complex with negligible electronic communication between the two Cu(II) centers. Cyclic voltammetry shows two sets of overlapping peaks at -0.33 V and -0.38 V corresponding to Cu(II)Cu(II)-Cu(II)Cu(I) and Cu(II)Cu(I)-Cu(I)Cu(I) indicating diffusion-controlled, quasireversible reaction accompanied by extensive structural reorganizations.

Keywords: Copper(II) mixed-carboxylates; one-pot synthesis; electronic structure; structure elucidation; liquid crystals

© 2020 Penerbit UTM Press. All rights reserved

INTRODUCTION

Metallomesogens (metal-based liquid crystals) involving transition metals have the combined advantage of anisotropy and fluidity of liquid crystals with useful properties associated with the presence of polarizable *d* electrons, such as tunable geometry and color, thermal stability, electronic conductivity, and magnetic and redox properties (Keerthiga, Kaliyappan, & Yoganandham, 2020; Therrien, 2020). Such metallomesogens are potential organic light emitting diode (Wang et al., 2016), thermoelectric material (Abdullah et al., 2016), catalyst (Meyyathal, Santhiya, Umadevi, Michelraj, & Ganesh, 2019), solar cell (Li et al., 2020) and optical device storage (Sunil et al., 2020).

Attard et al. (Attard & Cullum, 1990) reported that copper (II) carboxylates can promote the formation of discotic mesophase. This behavior is a consequence of the disc-like shapes of the polar cores of the molecules which consist of two copper (II) ions coordinated with four carboxylate groups. These dinuclear carboxylates have low magnetic moments due to the spin exchange between the unpaired electrons in each copper ion. It was suggested that the combination of discotic mesophase and the electronic properties of the dinuclear cores could lead to interesting conductance effect.

The discotic mesophase of copper (II) complexes of straight chain aliphatic carboxylates showed columnar stacks of the dimers with the columns arranged on a hexagonal lattice. The transition temperature between the crystalline phase and the columnar hexagonal mesophase ranges from 85°C to 120°C. The crankshaft appearance of the columnar, studied by Extended X-Ray Absorption Fine Structure (EXAFS), reveals weak bonds between the oxygen atoms of the carboxylate groups of one dimer and the free octahedral sites on the

copper ions in the neighboring dimer. These bonds are believed to further stabilize the complex. It has been reported that unsymmetrical compounds have lower melting points than symmetrical compounds, and that the clearing point increases when the chain length increase (Giroud-Godquin, 1998; Lacko, Papp, Szymańska, Szlyk, & Matejčík, 2018). For example, [Cu₂(CH₃(CH₂)₁₄COO)₄] has a melting temperature of 112 °C and clearing temperature of 220 °C, whereas [Cu₂((CH₂)₇CHCOO)₄] has the melting temperature of -20 °C and clearing temperature of 214 °C (Giroud-Godquin, 1998). Linear chains also enhance the anisotropy of the system and the fact that they are flexible and do not crystallize easily lead to lowering of their melting temperature (Simion et al., 2015).

Rao et al. (Singh et al., 2008) reported a mesogenic (nematic) Schiff-base of N,N''-di-4-(4''-pentylxybenzoate) salicylidenediaminoethane, H₂dpbsde (abbreviated as H₂L₅). The authors studied the mesogenic properties of H₂L₅ as well as [NiL₅]₂ and [CuL₅] complexes, using polarized optical microscopy and differential scanning calorimetry (DSC). The introduction of the metal ion into the metal-coordination sphere, as expected, resulted in the elevation of the transition temperature, melting and clearing points. The assignment of the mesophase (nematic) in each case was on the basis of the optical textures and the DSC thermograms. From DSC, the transition temperatures for the ligand (H₂L₁) were: crystal to nematic (crys-N), 175 °C; nematic to isotropic liquid (N-I), 229 °C; and isotropic liquid to nematic (I-N), 216 °C. For [NiL₅]₂, the transition temperatures were crys-crys, 145 °C; crys-N, 245 °C; and N-I (decompose), 255 °C; whereas for [CuL₅], crys-crys, 136 °C; crys-N, 225 °C; N-I, 261 °C; and N-crys, 200 °C.

Our current research interest is on thermally-stable and low-temperature functional metallomesogens and metal-based ionic liquids. Two strategies are adopted in designing the desired materials. The first is to induce self-assembly through the formation of H-bonds (for metallomesogens) or be ionized (for ionic liquids) by replacing at least one of the alkanooates with an aroate carrying an -OH or -NH₂ functional group. The second is to lower the melting temperature by lowering the molecular symmetry and by using ligands with long or non-linear alkyl chains. Our concept is based on copper (II) homocarboxylates, [Cu₂(μ-RCOO)₄], where R is a long linear (for metallomesogens) or branched hydrocarbon chain (for ionic liquids).

Our initial work is focusing on copper (II) mixed carboxylates with the general formula [Cu₂(p-XC₆H₄COO)₂(R'COO)₂], where X is a functional group that can form H-bond, such as -OH or -NH₂, and R' is a long linear hydrocarbon chain. The most challenging aspect of our work is the synthesis of the desired materials. Three synthetic methods were tried, namely metathesis, ligand-exchange and one-pot, and found that the latter method is most suitable for the intended mixed carboxylates.

In this paper, we report a one-pot synthesis of [Cu₂(p-H₂NC₆H₄COO)₂(CH₃(CH₂)₁₄COO)₂] (**Complex 1**). The complex was characterized by elemental analyses, Fourier transform infrared (FTIR) and UV-vis spectroscopies, thermogravimetry (TGA), differential scanning calorimetry (DSC), polarizing optical microscopy (POM), room-temperature magnetic susceptibility and cyclic voltammetry (CV). Currently to our knowledge, there is no report on the synthesis and characterization of this complex.

EXPERIMENTAL

Materials and instrumentations

Copper (II) nitrate trihydrate (Cu(NO₃)₂·3H₂O), palmitic acid (CH₃(CH₂)₁₄COOH), *p*-aminobenzoic acid (*p*-H₂NC₆H₄COOH), ethanol and ammonia were obtained from Merck. All chemicals were obtained from commercial sources and used as received. The elemental analyses were performed on a Thermo Finnigan Flash EA 1112. The FTIR spectrum was recorded using KBr disc in the 4000–400 cm⁻¹ region on a Perkin-Elmer FTIR SPECTRUM RX 1 spectrometer. The electronic spectrum was obtained on a Shimadzu UV-vis-NIR 3600 spectrophotometer. The TGA was recorded from 50–900 °C on a Perkin-Elmer Pyris Diamond TG/DTA Thermal System at a scan rate of 20 °C min⁻¹. The DSC was recorded from 35–300 °C on a Perkin-Elmer DSC 6 at a scan rate of 10 °C min⁻¹. Both thermal analyses were performed under N₂ at a flow rate of 10 cm³ min⁻¹. The POM was performed on an Olympus polarizing microscope equipped with a Mettler Toledo FP90 central processor and FN82HT hot stage. The heating and cooling rates were 3 °C min⁻¹ and the magnification was 20X. The room-temperature magnetic susceptibility was measured on a Sherwood Auto Magnetic Susceptibility Balance by the Gouy method, using Hg[Co(SCN)₄] as the calibrant. The molar susceptibility was corrected for the diamagnetism of the constituent atoms using Pascal's constants. The CV was performed on a Gamry Potentiostat/Galvanostat 600 instrument, using a standard three-electrode assembly (glassy carbon as the working electrode, platinum as the counter electrode, and Ag/AgCl as the reference electrode), and (nBu)₄NBF₄ (0.1 M) as the supporting electrolyte. The solvent was DMSO, the scan rate was 100 mV s⁻¹, and the quoted E values are versus Ag/AgCl.

Synthesis of Copper complex

An aqueous solution of Cu(NO₃)₂·3H₂O (23.4 mmol) was added to a mixture of *p*-H₂NC₆H₄COOH (23.6 mmol) and CH₃(CH₂)₁₄COOH (23.4 mmol) in hot ethanol. The green solution formed was cooled to room temperature with the addition of NH₃ dropwise to the magnetically stirred solution. The purple solution formed was left at room temperature for 12 hours, and then the excess NH₃ was removed by gentle heating. The product was a pale blue powder, and the yield was 34.2 %. Elemental Anal. Found: C, 59.24; H, 10.92, N, 2.48 %. Calcd. for Cu₂C₄₈H₈₂N₂O₁₀: C, 59.19; H, 8.43; N, 2.88 %. FTIR (KBr,

cm⁻¹): 3385-3300(w), 2913(vs), 2848(s), 1597(s), 1534(s), 1445(s), 1406(s), 716(s).

RESULTS AND DISCUSSION

Synthesis and elucidation of the structural formula

A facile one-pot reaction involving an equimolar ethanolic solution of Cu(NO₃)₂, *p*-H₂NC₆H₄COOH and CH₃(CH₂)₁₄COOH formed a pale blue powder upon neutralization with NH₃. The reaction involved self-assembly of Cu²⁺ ion with *p*-H₂NC₆H₄COO⁻ and CH₃(CH₂)₁₄COO⁻ ions generated *in situ* by NH₃ from the corresponding carboxylic acids.

The chemical formula of the pale blue powder, based on the elemental analyses, is Cu₂C₄₈H₈₂N₂O₁₀ (**Complex 1**). Based on the following arguments, it is proposed to have the structural formula [Cu₂(p-H₂NC₆H₄COO)₂(CH₃(CH₂)₁₄COO)₂(H₂O)(CH₃CH₂OH)] (**Figure 1**).

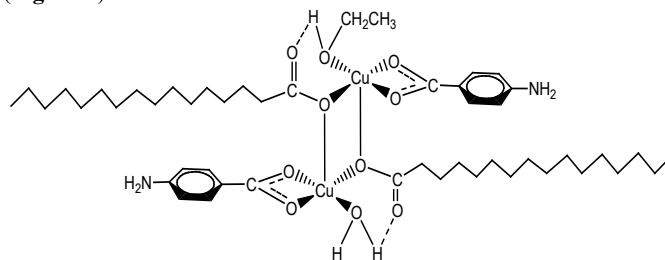


Figure 1. Proposed structure of **Complex 1**.

Complex 1 was soluble in ethanoic acid and pyridine, but insoluble in most other common polar and non-polar organic solvents. This is consistent with the presence of basic NH₂ group, and unavailable and/or sterically hindered axial sites at the two Cu(II) centers, respectively.

The FTIR spectrum (**Figure S1**) of **Complex 1** shows the presence of the expected functional groups based on the proposed structural formula, namely NH₂ at about 3200-3067 cm⁻¹ (Iliş & Cırcu, 2018), CH₂ at 2913 cm⁻¹ (asymmetrical stretching) and 2848 cm⁻¹ (symmetrical stretching), aromatic C-C at 1597 cm⁻¹, COO at 1597 and 1534 cm⁻¹ (asymmetrical stretching), 1445 and 1406 cm⁻¹ (symmetrical stretching), and *p*-substituted aromatic ring at 716 cm⁻¹. Accordingly, the ΔCOO values (ΔCOO = ν_{asym}COO - ν_{sym}COO) are 89 cm⁻¹ (chelating) and 191 cm⁻¹ (monodentate syn, antibridging) for the carboxylate ligands (Muhammad et al., 2019; Norazzizi Nordin, 2015; Zhou et al., 2019).

Optical properties

The molar conductivity (Λ_M) of **Complex 1**, was 21.2 S cm² mol⁻¹. The low value means that the complex is a non-electrolyte (Tavassoli et al., 2020). From this, it may be inferred that the complex did not dissociate to the corresponding ions in the mixed solvents. This fact is important when discussing the solution chemistry of the complex later. The electronic spectrum of **Complex 1** (**Figure 2(a)**) dissolved in DMSO (with a few drops of ethanoic acid added to increase its solubility) shows a broad *d-d* peak at 712 nm (ε = 485 M⁻¹ cm⁻¹) and a distinct shoulder at 359 nm (ε = 341 M⁻¹ cm⁻¹) superimposed on a strong charge-transfer band. The shoulder band is a characteristic of pentacoordinated binuclear complexes (Paschke, Balkow, & Sinn, 2002), in agreement with the proposed structure. Meanwhile, the solid state electronic spectrum of **Complex 1** (**Figure 2(b)**) shows two broad *d-d* bands at 656 nm (Band I) and 441 nm (Band II) with absorbance ratio ~ 3:1. This suggest either distorted square planar or square pyramidal binuclear Cu(II) complex (Batool, Gilani, Tahir, & Ruffer, 2017). Furthermore, the optical absorption threshold for the as-prepared **Complex 1** can be calculated based on the equation of E_g (eV) = 1240/λ, where E_g is the bandgap energy of the material (eV) and λ is the wavelength (nm) which give the bandgap energy of **Complex 1** of 1.7 eV and 1.9 eV in solution and solid condition, correspondingly (Mat et al., 2019).

The low bandgap energy suggests that the recombination process of charge carriers namely electrons and holes in **Complex 1** is efficient and could be a good candidate for other application such as in

photocatalyst. UV-Vis of the “precursors” of **Complex 1**, namely $[\text{Cu}_2(p\text{-H}_2\text{NC}_6\text{H}_4\text{COO})_4]$ and $[\text{Cu}_2(\text{CH}_3(\text{CH}_2)_{14}\text{COO})_4]$ have been investigated and tabulated in **Table 1**. Two deductions may be made from **Table 1**: (a) Band I of **Complex 1** is at intermediate energy between its “precursors”. This supports the presence of both aromatic and aliphatic carboxylates in the complex; and (b) Band II is at the same energy with the aromatic precursor, which are at lower energy compared to the aliphatic precursor. These suggests that the aromatic carboxylate is “closer” to Cu(II) compared to the aliphatic carboxylate or in the other hand, the aromatic carboxylate is less strongly coordinated (chelating) to Cu(II) compared to the aliphatic carboxylate (*syn-anti* bridging).

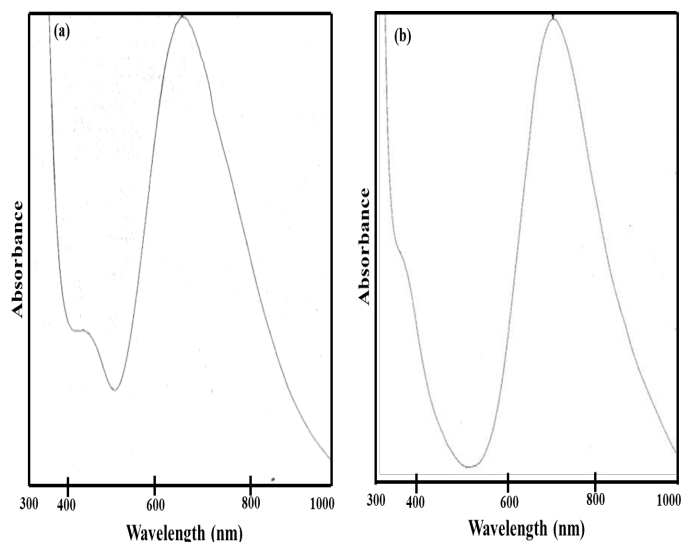


Figure 2. The UV-vis spectra of **Complex 1** in (a) solution; (b) solid state.

Table 1. Electronic spectroscopic data for 1 and its “precursors” in the solid state.

Complex	<i>d-d</i> Band (nm)		Absorbance ratio
	Band I	Band II	
1	656	441	3:1
$[\text{Cu}_2(p\text{-H}_2\text{NC}_6\text{H}_4\text{COO})_4]$	628	441	1:1
$[\text{Cu}_2(\text{CH}_3(\text{CH}_2)_{14}\text{COO})_4]$	674	383	3:1

Based on the discussed results, the proposed structural formula of **Complex 1** is shown in **Figure 1**. The proposed structure is consistent with the chemical formula $\text{Cu}_2\text{C}_{48}\text{H}_{82}\text{N}_2\text{O}_{10}$ (FW = 974.3 g mol⁻¹) as suggested the elemental analyses, and it shows *syn-anti* monodentate bridging $\text{CH}_3(\text{CH}_2)_{14}\text{COO}$ and chelating $p\text{-H}_2\text{NC}_6\text{H}_4\text{COO}$ as suggested from FTIR, and square pyramidal geometry at Cu(II) as suggested from UV-vis (local symmetries for the two Cu(II) is *CI*). The proposed structural formula is further supported by the crystal structure (**Figure 3**) of one of the products formed when **Complex 1** was reacted with 2,2'-bipyridine (**Complex 2**). The other product was identified as $[\text{Cu}_2(p\text{-H}_2\text{NC}_6\text{H}_4\text{COO})_4]$ based on its FTIR spectrum when compared with that of the aromatic “precursor”. The crystal was also obtained from the reaction of $[\text{Cu}_2(\text{CH}_3(\text{CH}_2)_{14}\text{COO})_4]$ with 2,2'-bipyridine.

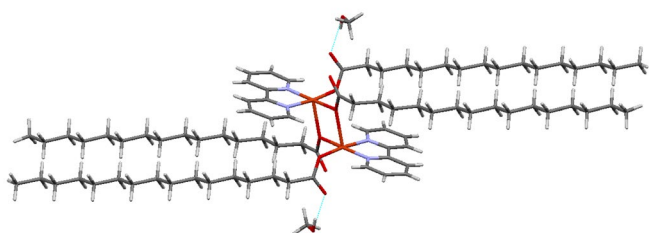


Figure 3. Crystal structure of **Complex 2**.

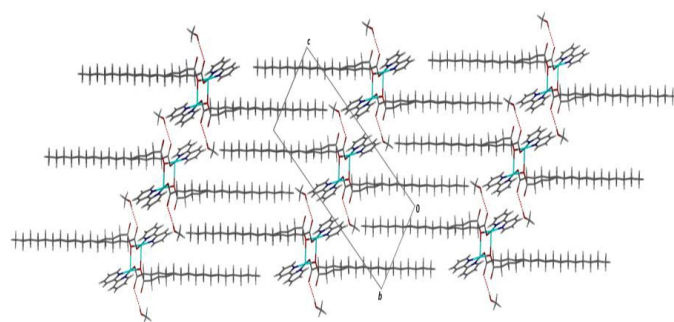


Figure 4. Packing pattern of **Complex 2**.

Thermal and mesogenic properties

The TGA trace of **Complex 1** (**Figure 5**) shows that it is thermally stable up to 256 °C. The initial weight loss from 100 °C to 117 °C (6.4 %) is due to the evaporation of H_2O and $\text{CH}_3\text{CH}_2\text{OH}$ molecules (expected 6.6 %). The total weight loss from 256 °C to 533 °C is 76.6 % and is assigned to the decomposition of the carboxylate ligands (expected 79.7 %) to CO_2 and other volatiles. The amount of residue at above 600 °C is 17.0 %. Assuming that it is CuO , the estimated formula mass of **Complex 1**, calculated using the gravimetry concept, is 936 g mol⁻¹ (expected 973 g mol⁻¹). Thus, the results from TGA and elemental analyses are in good agreement, and further support for the proposed structural formula.

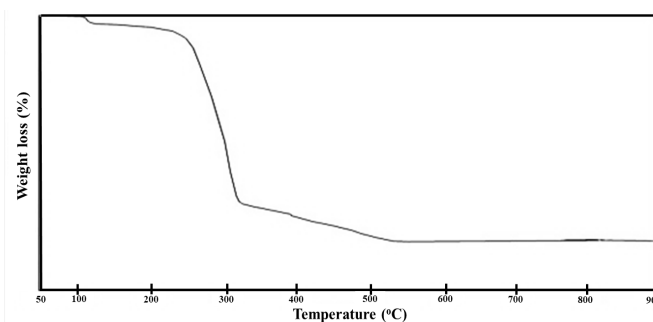


Figure 5. TGA of **Complex 1**.

From optical polarized microscope (OPM), **Complex 1** was observed to melt at 114 °C and then cleared to an isotropic liquid at 133 °C (**Figure 6(a)**). The color of the liquid darkened on further heating to temperatures below its decomposition temperature. On cooling from the isotropic liquid phase, a smectic C mesophase, SmC was observed at 82 °C (**Figure 6(b)**) and remained unchanged on further cooling to room temperature. The observed optical texture is as expected from the rod-like metallomesogen, consistent with the proposed structural formula. The darkening of color on heating was due to loss of H_2O and $\text{CH}_3\text{CH}_2\text{OH}$, which maximizes the intermolecular interaction and enables the development of the observed optical texture. The formation of mesophase at lower temperature in the present study than the melting point indicative of solid-liquid transition before the complex was fully melted at above 100 °C (Abdullah et al., 2016).

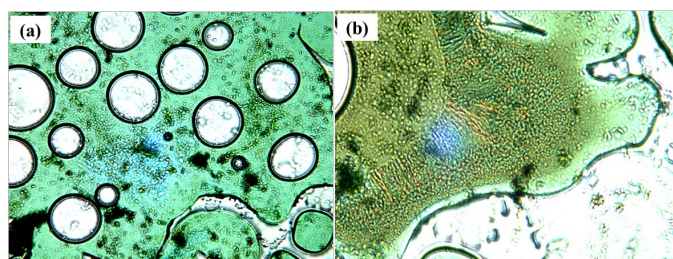


Figure 6. OPM image of **Complex 1** on (a) heating to 133 °C (clearing temperature) and (b) cooling to 82 °C.

The DSC of **Complex 1** (Figure 7) shows two strong overlapping endotherms at 110 °C and 119 °C ($\Delta H_{\text{combined}} = 229 \text{ kJ mol}^{-1}$) and broader overlapping endotherms centered at 264 °C ($\Delta H_{\text{combined}} = 121 \text{ kJ mol}^{-1}$). The lower temperature endotherms are assigned to the concurrent evaporation of H_2O and $\text{CH}_3\text{CH}_2\text{OH}$ molecules and melting of **Complex 1** respectively. The high enthalpy for these processes is consistent with the proposed structural formula, in which the solvent molecules are coordinated to Cu(II) and H-bonded to the ligands, and the presence of “intermolecular” interactions due to H-bond between two neighboring $p\text{-H}_2\text{NC}_6\text{H}_4\text{COO}$ ligands, and Van der Waals forces between $\text{CH}_3(\text{CH}_2)_{14}\text{COO}$ ligands. The higher temperature endotherms (above its decomposition temperature of 256 °C) are assigned to the decomposition of the carboxylate ligands to volatiles (mainly CO_2). Thus, the results of DSC and TGA are in good agreement, and consistent with the proposed structural formula.

Combining TGA, OPM and DSC results, the isotropic liquid range for **Complex 1** is 123 °C. This is significantly large when compared to $[\text{Cu}_2(\text{CH}_3(\text{CH}_2)_{14}\text{COO})_4]$, which decomposed immediately on clearing at 220 °C. Accordingly, **Complex 1** may be considered as a thermally-stable low-temperature thermotropic metallomesogen.

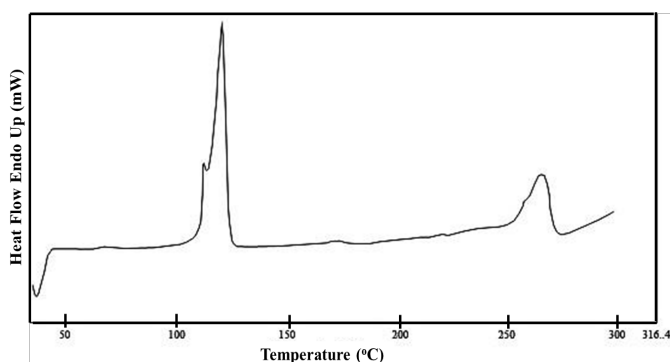


Figure 7. DSC of **Complex 1**.

Magnetic properties

The effective magnetic moment (μ_{eff}) of **Complex 1** at 298 K is 2.89 B.M. This value is calculated using the spin-only formula, $\mu_{\text{eff}} = 2.83[T(\chi_{\text{M}}^{\text{corr}} - N\alpha)]^{1/2}$, where T is the absolute temperature, $\chi_{\text{M}}^{\text{corr}}$ is the molar magnetic susceptibility corrected for diamagnetism of the constituent atoms, and $N\alpha$ is the temperature independent paramagnetism (120×10^{-6} cgs for a dicopper(II) complex). The μ_{eff} value is in excellent agreement with the presence of two unpaired electrons from two non-coupled Cu(II) ions (expected, 2.83 B.M.). Thus, it may be concluded that **Complex 1** is a paramagnetic dinuclear complex with negligible electronic communication between the two copper(II) centers. The observed magnetic property for **Complex 1** is in contrast with most Cu(II) carboxylates reported in the literature (Sosa, Ugalde-Saldívar, González, & Gasque, 2005). An example is $[\text{Cu}_2(\text{CH}_3(\text{CH}_2)_{14}\text{COO})_4]$ which has the value of 1.45 B.M. (calculated for monomer; expected 1.73 B.M.) (Attard & Cullum, 1990). The subnormal magnetic moment was ascribed to significant electronic coupling between the two Cu(II) centers, postulated to occur through the *syn-syn* bridging ligands (the superexchange pathway) of the paddle-wheel dimer.

However, our result is in tandem with the proposed structural formula, and with that reported by Konar et al. for $[\text{Cu}(\text{pyrazine-2,3-dicarboxylate})(\text{H}_2\text{O})_2] \cdot \text{H}_2\text{O}$, which also has the *syn-anti* carboxylate bridge (Konar, Manna, Zangrando, & Chaudhuri, 2004). These authors suggested that the almost negligible coupling between the Cu(II) centers in their complex was because of the reduction of the magnetic pathway as the basal ligand was well directed ($d_{x^2-y^2}$ magnetic orbital) but the axial ligand was unfavorably located (d_{z^2} orbital).

Electrochemical properties

The CV of **Complex 1** (Figure 8), scanned cathodically from 0 V (potential range -1.3 to +0.8 V), shows overlapping cathodic peaks at -

0.47 and at about -0.77 V (shoulder), and overlapping anodic peaks at -0.006 and at about +0.18 V (shoulder). Also observed is the nucleation overpotential at -1.1 V, characteristic of a nucleation growth mechanism (Sosa et al., 2005).

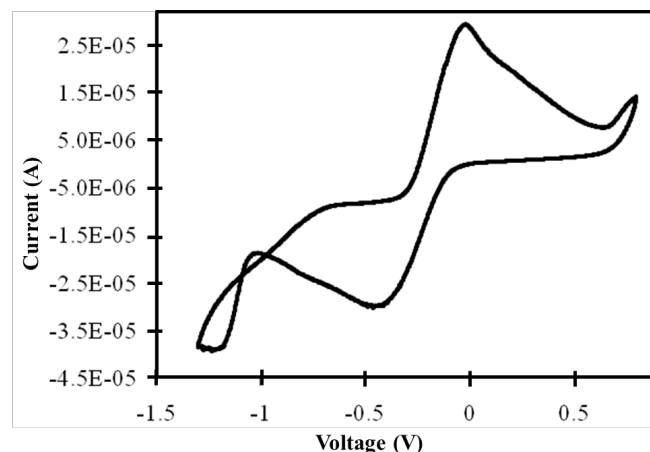


Figure 8. CV of **Complex 1** measured from -1.3 V to +0.8 V.

The overlapping peaks suggest two Cu(II) centers with negligible electronic interaction, which is consistent with its magnetic properties. The values of the two half-wave potentials, $E_{1/2}^1$ and $E_{1/2}^2$, are -0.33 V and -0.38 V respectively. These values are in good agreement with the value of -0.37 V reported for $[\text{Cu}(\text{CH}_3\text{COO})_2(2,2'\text{-bipy})]$ (Mohamadine & Abdullah, 2010). The redox reactions are summarized below.



The difference between the half-wave potentials of the two redox processes (ΔE) is a measure of the relative stability of the mixed-valence species ($\text{Cu}_2^{\text{II,I}}$). This is related to the comproportionation constant, K_{con} , calculated using the relationship: $\log K_{\text{con}} = \Delta E/0.0591$. Accordingly, the value of K_{con} for **Complex 1** is 7, which suggests that the mixed-valence species is very unstable, consistent with the negligible exchange interaction between the two Cu(II) centres. The peaks separation ($E_{\text{pc}} - E_{\text{pa}}$) are 650 and 764 mV, and the corresponding anodic to cathodic peak currents ratios ($i_{\text{pa}}/i_{\text{pc}}$) are 1.2 and 1.0 respectively. From these, it may be suggested that **Complex 1** underwent quasi-reversible, diffusion-controlled electrochemical reactions followed by extensive structural reorganization. However, it is noted that there is no large anodic feature on the reverse scan, indicating that the $\text{Cu}_2^{\text{I,I}}$ species is stabilized towards further reduction or disproportionation to Cu, expected to occur at about -0.9 V (Mohamadine & Abdullah, 2010).

The electrochemical behavior of **Complex 1** was further probed by recording its CV in a wider potential range (-1.5 to +1.0 V; Figure S2). It is noted that the metal-based redox peaks remained at about the same potentials. However, for the larger potential range, there is an additional cathodic peak at -1.23 V, and two additional anodic peaks at +0.44 and +0.88 V.

To correctly assign the new peaks, the CV for its “precursor”, $[\text{Cu}_2(p\text{-H}_2\text{NC}_6\text{H}_4\text{COO})_4]$ and $[\text{Cu}_2(\text{CH}_3(\text{CH}_2)_{14}\text{COO})_4]$ were recorded under the same conditions (not shown). The CV for $[\text{Cu}_2(p\text{-H}_2\text{NC}_6\text{H}_4\text{COO})_4]$ shows two cathodic peaks at -0.62 and -1.46 V, three overlapping anodic peaks at +0.14, +0.35, and +0.48 V, and another anodic peak at +1.44 V. In contrast, the CV for $[\text{Cu}_2(\text{CH}_3(\text{CH}_2)_{14}\text{COO})_4]$ shows a cathodic peak at -0.83 V and two anodic peaks at -0.26 and +1.45 V.

The new cathodic peak at -1.23 V and new anodic peak at +0.44 V for **Complex 1** are in common only with $[\text{Cu}_2(p\text{-H}_2\text{NC}_6\text{H}_4\text{COO})_4]$ (-1.46 and +0.48 V). Accordingly, these peaks are assigned to the reduction and oxidation of $p\text{-H}_2\text{NC}_6\text{H}_4\text{COO}$ ligand. The new anodic peak at +0.88 V for **Complex 1** is in common with that of $[\text{Cu}_2(p\text{-H}_2\text{NC}_6\text{H}_4\text{COO})_4]$ and $[\text{Cu}_2(\text{CH}_3(\text{CH}_2)_{14}\text{COO})_4]$ (~+1.44 V). Thus, this peak is tentatively assigned to the oxidation of -COO fraction of the

carboxylate ligands. It is probable that the more facile oxidation for **Complex 1** compared to both of its “precursors” is due to the difference in their structure (*syn-anti* versus *syn-syn* bridging mode).

CONCLUSION

[Cu₂(p-H₂NC₆H₄COO)₂(CH₃(CH₂)₁₄COO)₂(H₂O)(CH₃CH₂OH)] is a new dicopper(II) mixed-carboxylate complex formed in a facile one-pot self-assembly reaction of the corresponding ions. It is a low-temperature, thermally-stable, paramagnetic, and redox-active thermotropic metallomesogen with wide isotropic temperature range.

ACKNOWLEDGEMENT

This work was financially supported by the Universiti of Malaya under the Research University Grant and Ministry of Higher Education Malaysia.

REFERENCES

- Abdullah, N., Mohd Said, S., Halid, Y. Y., Megat Hasnan, M. M. I., Sharmin, N., Mat Hussin, S. A., . . . Anuar, N. S. (2016). Complexes of nickel (II) carboxylates with pyridine and cyclam: crystal structures, mesomorphisms, and thermoelectrical properties. *Journal of Coordination Chemistry*, 69(19), 2954-2971.
- Attard, G., & Cullum, P. (1990). Thermotropic mesomorphism in a branched chain copper (II) carboxylate and its pyrazine complex. *Liquid Crystals*, 8(3), 299-309.
- Batool, S. S., Gilani, S. R., Tahir, M. N., & Ruffer, T. (2017). Synthesis, and structural characterization of mixed ligand copper (II) complexes of N,N,N',N'-tetramethylethylenediamine incorporating carboxylates. *Journal of Molecular Structure*, 1148, 7-14.
- Giroud-Godquin, A. M. (1998). My 20 years of research in the chemistry of metal containing liquid crystals. *Coordination Chemistry Reviews*, 178, 1485-1499.
- Iliş, M., & Cîrcu, V. (2018). Discotic liquid crystals based on Cu (I) complexes with benzoylthiourea derivatives containing a perfluoroalkyl chain. *Journal of Chemistry*, 2018.
- Keerthiga, R., Kaliyappan, T., & Yoganandham, S. T. (2020). Study on synthesis and investigation of supramolecular cuperic (Cu (II)) metallomesogens with Smectic C phase. *Inorganic Chemistry Communications*, 107954-107960.
- Konar, S., Manna, S. C., Zangrando, E., & Chaudhuri, N. R. (2004). Crystal structure and magnetic behavior of a copper (II)-(pyrazine-2,3-dicarboxylate) coordination polymer: 3D architecture stabilized by H-bonding. *Inorganica Chimica Acta*, 357(5), 1593-1597.
- Lacko, M., Papp, P., Szymańska, I. B., Szlyk, E., & Matejčík, Š. (2018). Electron interaction with copper (II) carboxylate compounds. *Beilstein journal of nanotechnology*, 9(1), 384-398.
- Li, X., Zhao, Z., Zhou, J., Wang, C., Wu, Y., & Tan, S. (2020). An all-solid-state lamellar-nanostructured polymer electrolyte in-situ-prepared from smectic liquid crystal for thermally stable dye-sensitized solar cells. *Chemical engineering science*, 115710.
- Mat, A. N. C., Sairi, N. A., Basirun, W. J., Rezayi, M., Teridi, M. A. M., & Mazhar, M. (2019). Photoelectrocatalytic oxidation of methanol over RuO₂-MnO₂-Co₃O₄ supported porous anatase under visible light irradiation. *Materials Chemistry and Physics*, 224, 196-205.
- Meyyathal, P., Santhiya, N., Umadevi, S., Michelraj, S., & Ganesh, V. (2019). Lyotropic liquid crystal directed synthesis of anisotropic copper microparticles and their application in catalysis. *Colloids and Surfaces A: Physicochemical and Engineering Aspects*, 575, 237-244.
- Mohamadin, M., & Abdullah, N. (2010). Thermal stability and electrochemical behaviour of Tetrakis-μ-benzoatodicopper (II). *Open Chemistry*, 8(5), 1090-1096.
- Muhammad, N., Ikram, M., Perveen, F., Ibrahim, M., Ibrahim, M., Rehman, S., . . . Schulzke, C. (2019). Syntheses, crystal structures and DNA binding potential of copper (II) carboxylates. *Journal of Molecular Structure*, 1196, 771-782.
- Norazzizi Nordin, W. Z. S., Muhammad Rahimi Yusop, Mohamed Rozali Othman. (2015). Synthesis and characterization of copper (II) carboxylate with palm-based oleic acid by electrochemical technique. *Malaysian Journal of Analytical Sciences*, 19(1), 236-243.
- Paschke, R., Balkow, D., & Sinn, E. (2002). Lowering melting points in asymmetrically substituted Salen-copper(II) complexes exhibiting mesomorphic behavior. Structure of the mesogen Cu(5-hexyloxySalen). *Inorganic Chemistry*, 41(7), 1949-1953.
- Simion, A., Huzum, C.-C., Carlescu, I., Lisa, G., Balan, M., & Scutaru, D. (2015). Unsymmetrical banana-shaped liquid crystalline compounds 1 derived from 2,7-dihydroxynaphthalene. *Journal of the Serbian Chemical Society*, 80(5), 673-683.
- Singh, A. K., Kumari, S., Row, T. G., Prakash, J., Kumar, K. R., Sridhar, B., & Rao, T. (2008). Coordination of a mesogenic Schiff-base with Mn(II), Co(II), Ni(II), Cu(II) and Zn(II): Synthesis, spectral studies and crystal structures. *Polyhedron*, 27(18), 3710-3716.
- Sosa, A. M., Ugalde-Saldívar, V. M., González, I., & Gasque, L. (2005). Electrochemical studies of a dinuclear copper complex with imidazole derivative ligand H₃bphenim. *Journal of Electroanalytical Chemistry*, 579(1), 103-111.
- Sunil, B., Srinatha, M., Shanker, G., Hegde, G., Alaasar, M., & Tschierske, C. (2020). Effective tuning of optical storage devices using photosensitive bent-core liquid crystals. *Journal of Molecular Liquids*, 304, 112719.
- Tavassoli, M., Montazerzohori, M., Naghiha, R., Sadeghi, H., Masoudiasl, A., Jooari, S., . . . Mahmoudi, G. (2020). Some new nanostructure zinc complex: Synthesis, spectral analyses, crystal structure, Hirshfeld surface analyses, antimicrobial/anticancer, thermal behavior and usage as precursor for ZnO nanostructure. *Materials Science and Engineering: C*, 110, 110642.
- Therrien, B. (2020). Thermotropic liquid-crystalline materials based on supramolecular coordination complexes. *Inorganics*, 8(1), 2.
- Wang, Y., Fan, J., Shi, J., Qi, H., Baranoff, E., Xie, G., . . . Zhu, W. (2016). Influence of integrated alkyl-chain length on the mesogenic and photophysical properties of platinum-based metallomesogens and their application for polarized white OLEDs. *Dyes and Pigments*, 133, 238-247.
- Zhou, Y.-D., Ma, J., Ren, G.-C., Gao, G.-R., Fu, K.-X., Chang, S.-J., . . . Deng, Y.-H. (2019). First transition metal complex containing SMIA-carboxylate ligand: Synthesis, structure and magnetic properties of a new tetranuclear copper complex [Cu₄(SMIA)₆(phen)₄](ClO₄)₂. *Inorganic Chemistry Communications*, 102, 152-157.